Measurement of dynamic and static radiation force on a sphere

Shigao Chen*
Department of Physiology and Biomedical Engineering, Mayo Clinic College of Medicine, Rochester, Minnesota 55905, USA

Glauber T. Silva
Department of Information Technology, Universidade Federal de Alagoas, Campus A.C., Simões-BR 104-KM 14, Maceio, AL, Brasil

Randall R. Kinnick, James F. Greenleaf, and Mostafa Fatemi
Department of Physiology and Biomedical Engineering, Mayo Clinic College of Medicine, Rochester, Minnesota 55905, USA
(Received 28 September 2004; revised manuscript received 15 December 2004; published 26 May 2005)

Dynamic radiation force from ultrasound has found increasing applications in elasticity imaging methods such as vibro-acoustography. Radiation force that has both static and dynamic components can be produced by interfering two ultrasound beams of slightly different frequencies. This paper presents a method to measure both static and dynamic components of the radiation force on a sphere suspended by thin threads in water. Due to ultrasound radiation force, the sphere deflects to an equilibrant position and vibrates around it. The static radiation force is estimated from the deflection of the sphere. The dynamic radiation force is estimated from the calculated radiation impedance of the sphere and its vibration speed measured by a laser vibrometer. Experimental results on spheres of different size, vibrated at various frequencies, confirm the theoretical prediction that the dynamic and static radiation force on a sphere have approximately equal magnitudes [G. T. Silva *et al.*, Phys. Rev. E **71**, 056617 (2005)].

DOI: 10.1103/PhysRevE.71.056618 PACS number(s): 43.58.+z, 43.25.+y, 43.20.+g

I. INTRODUCTION

Acoustic radiation force is a phenomenon associated with the nonlinear nature of acoustic wave propagation in a medium. The force is caused by the transfer of momentum from the wave to an object in the wave path. In an attenuating medium, part of the wave momentum is transferred to the medium, resulting in a force exerted on the medium along the direction of the wave propagation. The magnitude of the radiation force exerted on an object by a wave depends upon both the medium's mechanical characteristics and the object scattering properties.

Commonly, the acoustic radiation force is defined as a steady force, given that the intensity of the incident sound field does not change over time. It has been shown that radiation force can have both a static and a dynamic (oscillatory) component, if the intensity of the incident field is modulated versus time. This can be achieved either by the interference of two sound beams with identical amplitude but slightly different frequencies or, equivalently, by a suppressed-carrier amplitude modulated (SCAM) beam [1].

Recently, the dynamic ultrasound radiation force has found increasing applications in elasticity imaging techniques. For example, vibro-acoustography [2] uses dynamic radiation force from focused ultrasound to vibrate an object at audio frequencies and makes images related to the object's elasticity from its acoustic emissions. This technique has been successfully used to image artery calcifications [3], breast microcalcifications [4,5], calcium deposit on heart valves [2], human calcaneus and hip [6], and brachytherapy metal seeds [7]. In addition, dynamic radiation force from ultrasound was also used to generate shear waves in a medium, from which its shear modulus and viscosity can be estimated [8]. Other applications of dynamic radiation force include determining resonance frequencies of differently shaped objects [9] and evaluating an artery's stiffness [10].

Despite the extensive use of dynamic radiation force, little work has been done on it theoretically and experimentally. Recently, the theory of dynamic radiation force on a solid cylinder immersed in ideal fluid was reported [11]. In another paper [12], the theory of dynamic radiation force on an object of arbitrary shape was developed. In particular, special attention has been paid to the dynamic radiation force on spheres because traditionally spherical targets have been the focus of theoretical [13–15] and experimental studies [16,17] of static radiation force. However, no experimental study on the dynamic radiation force has even been reported. In this paper, we present a method to measure the radiation force on a sphere suspended in water due to a SCAM ultrasound beam. The static component of the radiation force is estimated from the deflection of the sphere, whereas the dynamic component is derived from the sphere's vibration speed measured by optical vibrometry. Experimental results on several spheres of different radii demonstrate that the magnitude of the static and dynamic radiation force on the sphere is about the same, which confirms one of the theoretical predictions presented in [12].

II. METHOD

Figure 1(a) shows a sphere suspended with bifilar arrangement in water. Figure 1(b) is another projection of the sphere viewed from the right side of Fig. 1(a). An amplitude-

*Email: chen.shigao@mayo.edu

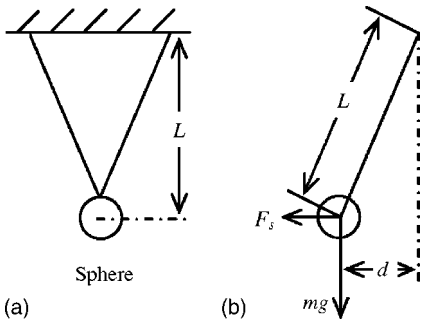

FIG. 1. The suspension and force balance on a sphere in a sound field.

modulated ultrasound propagates from the right side of Fig. 1(b) to the sphere. The static radiation force deflects the sphere to a new equilibrium position along the ultrasound beam. The dynamic radiation force causes the sphere to vibrate around this new equilibrium position.

A. Measurement of static radiation force

The vibration amplitude of the sphere is very small (e.g., less than 1 μm from the equilibrium position) in typical applications presented in this paper. Therefore, one can neglect the motion of the sphere when analyzing the balance of static forces on it. As shown in Fig. 1(b), the static radiation force F_s is balanced by the gravitational force on the sphere mg and the tension of the thread. Neglecting the mass of the thread, the displacement d of the sphere is related to the static radiation force as [17]

$$F_s = \frac{mgd}{\sqrt{L^2 - d^2}}, \tag{1}$$

where L is the suspension length, g is the acceleration due to gravity, and m is the mass of the sphere corrected for buoyancy. The buoyancy on the sphere is equal to the weight of water with identical volume as that of the sphere. Therefore, Eq. (1) can be rewritten as

$$F_s = \frac{4}{3}\pi a^3(\rho_s - \rho_w)g\frac{d}{\sqrt{L^2 - d^2}}, \tag{2}$$

where a is the radius of the sphere and ρ_s and ρ_w are the densities of the sphere and water, respectively. Therefore, the static radiation force on the sphere can be solved with Eq. (2), given that the deflection d can be measured accurately.

B. Measurement of dynamic radiation force

For a rigid sphere oscillating at radial frequency ω within a medium, the stress field around the sphere can be calculated. The net force on the sphere can be found by integrating the stress at the surface of the sphere. The radiation impedance of the sphere is defined as the net force divided by the vibrating speed of the sphere, and represents the resistance the sphere has to overcome when pushing its surrounding medium back and forth. The radiation impedance Z_r of an oscillating sphere in water is [18]

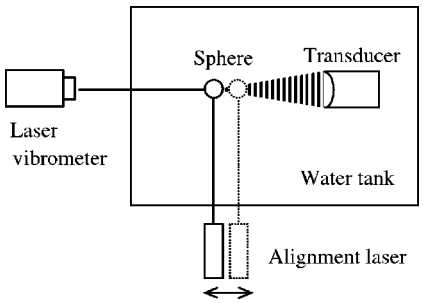

FIG. 2. The diagram of experimental setup. Ultrasound radiation force deflects and vibrates the sphere. The vibration is detected by the laser vibrometer. The deflection is measured by the alignment laser positioned on a micro-station.

$$Z_r = i\tfrac{4}{3}\pi a^3\rho_w\omega(2 + a^2k^2 - a^3k^3i)/(4 + a^4k^4), \tag{3}$$

where k is the wave number of the acoustic radiation. For typical applications in this paper, a is at the order of millimeter, while k is at the order of unity. Therefore, $ka \ll 1$ and Eq. (3) can be simplified to

$$Z_r = i\tfrac{2}{3}\pi a^3\rho_w\omega. \tag{4}$$

For a sphere of mass m and oscillating at velocity $Ve^{i\omega t}$, the force required to overcome the inertia of the sphere is

$$F = m\frac{d(Ve^{i\omega t})}{dt} = im\omega Ve^{i\omega t}. \tag{5}$$

We define the mechanical impedance Z_m of the sphere as

$$Z_m = \frac{F}{Ve^{i\omega t}} = im\omega = i\frac{4}{3}\pi a^3\rho_s\omega. \tag{6}$$

The dynamic radiation force drives the sphere to vibrate, while the impedances represent the resistance towards vibration. Dividing the driving force by the impedances yields the vibrating speed V of the sphere

$$V = \frac{F_d}{Z_r + Z_m}, \tag{7}$$

where F_d is the dynamic radiation force on the sphere. Substitution of Eqs. (4) and (6) into Eq. (7) yields

$$F_d = i\tfrac{4}{3}\pi a^3(0.5\rho_w + \rho_s)\omega V. \tag{8}$$

This result is essentially identical to Eq. 8 given by Ref. [19]. Equation (8) can be used to solve for the dynamic radiation force on the sphere, given that the vibration speed V of the sphere can be measured accurately.

III. EXPERIMENTS

Three 440C stainless spheres of radius 0.638, 0.851, and 1.19 mm are used in the experiments shown in Fig. 2. Each sphere is suspended with human hair (about 0.07 mm in diameter) in a bifilar arrangement. A 35 mm diameter flat piston transducer with an acoustic lens is used to insonify the sphere with CW (continuous wave) amplitude-modulated ultrasound. The distance between the transducer and the sphere

is about 10 cm and the center frequency of the insonation is 0.93 MHz. The ultrasound's beam width is relatively large such that its intensity does not change significantly across the sphere's surface.

The vibration of the sphere is detected by a laser vibrometer (Polytec GmbH, Waldbronn, Germany), which is aligned with the beam axis of the ultrasound transducer. There are a few details that require special attention in order to make correct measurements for these experiments. First, the Polytec laser is calibrated in air, while measurements on spheres are made in water. The speed, and hence the wavelength, of light in air are larger than that in water by a factor of 1.33. Therefore, for the same amount of motion, the Doppler frequency shift in water is 1.33 times larger than that in air. Consequently, the measurement made in water should be divided by 1.33 because the Polytec vibrometer measures vibration from the Doppler frequency shift of the reflected laser. Second, the "velocity range" (which also controls the highest detectable frequency) and the "velocity filter" (a low-pass filter) on the vibrometer should be set to as low as possible, to avoid aliasing from the motions at ultrasound frequency. In these experiments, they were set to $1\ \mathrm{mm\ s^{-1}}\ v^{-1}$ (with a highest detectable frequency of 10 kHz) and 5 kHz (cutoff frequency for the low-pass filter), respectively. Oscillations due to dynamic radiation force had frequencies less than 1 kHz, thus were detected by the laser vibrometer. In contrast, the vibrations at ultrasound frequency were cut off from the output.

The deflection of the sphere is measured with an alignment laser that is perpendicular to the ultrasound beam. The laser is first focused on the sphere at its deflection position. Then the ultrasound is turned off and the position of the laser is moved laterally on a micro-platform to align with the sphere at its rest position. The deflection of the sphere can thus be measured with 10 μm resolution.

IV. RESULTS

Each sphere is tested at three different vibration frequencies: 100, 200, and 400 Hz. This is achieved by changing the modulation frequency on the amplitude of a 0.93 kHz ultrasound. As an example, the detailed results on the smallest sphere vibrated at 100 Hz are presented here. The parameters of the sphere are $a=0.638$ mm, $\rho_s=7670\ \mathrm{kg\ m^{-3}}$, $\rho_w=1000\ \mathrm{kg\ m^{-3}}$, $g=9.81\ \mathrm{m\ s^{-2}}$, $L=61$ mm, $d=3.025$ mm, and $\omega=2\pi\times 100\ \mathrm{rad\ s^{-1}}$, $V=0.587\ \mathrm{mm\ s^{-1}}$ (already corrected by the factor of 1.33 for water). Substitution of these parameters into Eqs. (2) and (8) yields $F_s=3.45\times10^{-6}$ N, and $F_d=3.27\times10^{-6}$ N. The percentage difference between the measured static and dynamic radiation force is $|F_d-F_s|/0.5(F_d+F_s)=5.3\%$. For a vibration frequency of 200 Hz, the measurements on the same sphere yields $F_s=3.46\times10^{-6}$ N and $F_d=3.27\times10^{-6}$ N, with a 5.6% difference. At 400 Hz, the results are $F_s=3.53\times10^{-6}$ N and $F_d=3.34\times10^{-6}$ N, with a 5.3% difference.

The incident acoustic fields on the spheres were also measured to calculate the theoretical values of the dynamic and static radiation force on the sphere and compared with the experimental results. The transducer in Fig. 2 was operating at amplitude-modulated (AM) mode with suppressed carrier. The center frequency of the carrier was 0.93 MHz. This AM beam is equivalent to two ultrasound beams with identical amplitude, but with slightly different frequency, denoted by a and b. The radiation force on the sphere can be calculated with Eq. (42) of Ref. [12]. It is repeated here as Eq. (9) for the reader's convenience:

$$F_s = \pi a^2(E_a Y_a + E_b Y_b), \tag{9a}$$

$$F_d = \pi a^2 E_{\Delta\omega} Y_{\Delta\omega}, \tag{9b}$$

where $E_a=0.5\rho_w(k_aA^2)$, $E_b=0.5\rho_w(k_bA^2)$, $E_{\Delta\omega}=\rho_w k_a k_b A^2$, and Y_a, Y_b, and $Y_{\Delta\omega}$ are the static radiation force function at ultrasound frequencies a, b, and the dynamic radiation force function at acoustic frequency $\Delta\omega$, respectively. In these formulas, k_a and k_b are wave numbers corresponding to ultrasound frequencies a and b, and A represents the amplitude of the velocity potential. For a monochromatic plane wave, the amplitude of velocity potential A can be determined from the acoustic pressure amplitude p by $A=p/\rho kc$, where ρ, k, and c are the density, wave number, and sound speed of water, respectively. The incident acoustic pressure from the transducer was measured with a calibrated membrane hydrophone to be $p_a=p_b=83.74$ kPa. In these experiments, the difference frequencies are very small compared to the center frequency of the ultrasound. Therefore, Y_a, Y_b, and $Y_{\Delta\omega}$ should be almost identical and independent of the difference frequency. For the 0.638 mm radius sphere, the theory has $Y_a\approx Y_b\approx Y_{\Delta\omega}\approx 0.862$. From Eq. (9), the theoretical values for the static and dynamic radiation force on this sphere are $F_s\approx F_d\approx 3.51\times10^{-6}$ N. This theoretical value is very close to the measurement results reported above.

The incident acoustic pressure measured by the membrane hydrophone is not necessary equal to the actual acoustic pressure the sphere experiences. This can be due to two reasons. First, the incident acoustic wave is not a uniform plane wave, but rather has a nonuniform beam pattern (although this pattern is relatively flat). Thus the pressure on the sphere depends on its transverse position within the beam pattern. Second, there may be a standing wave between the transducer and the sphere, which will make the actual pressure on the sphere sensitive to its axial position [20]. For these two reasons, the incident pressures on each measurement may be different due to their different positioning within the beam pattern. Since the radiation force is related to the square of the incident pressure, the pressure inconsistency is amplified in radiation force. We found that the measured static and dynamic radiation force varied more for repeated measurements on larger spheres. This may be due to stronger standing wave effect for larger spheres. However, the measured magnitude of the static and dynamic radiation force for the larger spheres remained very close to each other in all measurements. This observation supports our hypothesis that the variations in radiation force measurements are mainly due to the variance of the actual incident pressure. Therefore, results for other spheres are reported as the percentage differences between F_s and F_d as shown in Table I. Calculating the percentage difference cancels variation due to incident pressure. The data in Table I confirm a theoretical

TABLE I. The percentage difference between dynamic and static radiation force measured at 100, 200, and 400 Hz for spheres of different radius.

	$a=0.638$ mm	$a=0.851$ mm	$a=1.19$ mm
100 Hz	5.3%	1.46%	0.98%
200 Hz	5.6%	2.1%	1.46%
400 Hz	5.3%	2.5%	1.61%

result in Ref. [12] stating that the dynamic and static radiation force on the sphere have equal magnitudes.

V. DISCUSSION

This study demonstrates the feasibility of using the deflection and vibration speed of a suspended sphere to measure the static and dynamic radiation force on the sphere. There are a number of limitations on this research. First of all, the influence of the thin thread and adhesive (used to attach the thread to the sphere) is not considered. Their weight can affect the static radiation force measurement, while the thread can change the radiation impedance of the sphere. These influences may be negligible for large spheres, but can be significant for small spheres. This may explain why the percentage differences in Table I are larger for smaller spheres. Second, acoustic streaming is neglected in this study. The pressure of the incident ultrasound used in the experiments is about 6×10^4 Pa. Using the method of Nyborg [21], the acoustic streaming is estimated to be less than 1 mm s^{-1} in water. The drag on the sphere by the streaming can be calculated by Stoke's formula [22]. It is at the order of 10^{-8} N, which is about 1% of the radiation force measured on the sphere. Therefore, the effect of acoustic streaming on the radiation force measurements can be safely neglected.

The measurement of dynamic radiation force can be extended to a sphere embedded in viscoelastic medium. The radiation impedance formula for a sphere in viscoelastic medium derived by Oestreicher [18] should be used to replace Eq. (3). Two new unknown parameters (shear elasticity and viscosity of the medium) needed in the new radiation impedance formula can be estimated from the resonance of the sphere [19]. The method described here can be readily adapted to geometries other than a sphere, such as a rectangular or circular disk.

VI. CONCLUSIONS

This paper presents a method to measure both static and dynamic radiation force on a sphere suspended by thin threads in water. Radiation force that has a dynamic component can be produced by interfering two ultrasounds of slightly different frequency, or by a single ultrasound beam whose amplitude is modulated at a low frequency. The sphere deflects to an equilibrant position and vibrates around it. The static radiation force is estimated from the deflection of the sphere. The dynamic radiation force is estimated by measuring the vibration velocity of the sphere. Experiments on spheres of different size, vibrated at various frequencies, show that the magnitudes of static and dynamic radiation forces on each sphere are very similar, with less than 6% difference. This is in accordance with a theory which states that the static and dynamic radiation force on a sphere should have identical magnitude for suppressed carrier AM ultrasound.

ACKNOWLEDGMENTS

This work is supported by Grant Nos. EB02167 and EB00535 from National Institute of Health.

[1] S. Chen, M. Fatemi, R. R. Kinnick, and J. F. Greenleaf, IEEE Trans. Ultrason. Ferroelectr. Freq. Control **51**, 313 (2004).
[2] M. Fatemi, A. Manduca, and J. F. Greenleaf, Proc. IEEE **91**, 1503 (2003).
[3] M. Fatemi and J. F. Greenleaf, Phys. Med. Biol. **45**, 1449 (2000).
[4] M. Fatemi, L. E. Wold, A. Alizad, and J. F. Greenleaf, IEEE Trans. Med. Imaging **21**, 1 (2002).
[5] A. Alizad, M. Fatemi, L. E. Wold, and J. F. Greenleaf, IEEE Trans. Med. Imaging **23**, 307 (2004).
[6] S. Callé, J. P. Remenieras, O. Bou Matar, and F. Patat, Ultrasound Med. Biol. **29**, 465 (2003).
[7] F. Mitri, P. Trompette, and J. Y. Chapelon, IEEE Trans. Med. Imaging **23**, 1 (2004).
[8] S. Chen, M. Fatemi, and J. F. Greenleaf, J. Acoust. Soc. Am. **115**, 2781 (2004).
[9] F. Mitri, P. Trompette, and J. Y. Chapelon, J. Acoust. Soc. Am. **114**, 2648 (2003).
[10] X. Zhang, R. R. Kinnick, M. Fatemi, and J. F. Greenleaf, Proc. 2003 IEEE Ultrason. Symp. 1883.
[11] F. G. Mitri and S. Chen, Phys. Rev. E **71**, 016306 (2005).
[12] G. T. Silva, S. Chen, J. F. Greenleaf, and M. Fatemi, Phys. Rev. E **71**, 056617 (2005).
[13] W. L. Nyborg, J. Acoust. Soc. Am. **42**, 947 (1967).
[14] T. Hasegawa and K. Yosioka, J. Acoust. Soc. Am. **46**, 1139 (1969).
[15] T. Hasegawa and Y. Watanabe, J. Acoust. Soc. Am. **63**, 1733 (1978).
[16] T. Hasegawa and K. Yosioka, J. Acoust. Soc. Am. **58**, 581 (1975).
[17] F. Dunn, A. J. Averbuch, and W. D. O'Brien, Acustica **38**, 58 (1977).
[18] H. L. Oestreicher, J. Acoust. Soc. Am. **23**, 707 (1951).
[19] S. Chen, M. Fatemi, and J. F. Greenleaf, J. Acoust. Soc. Am. **112**, 884 (2002).
[20] A. Alizad, M. Fatemi, L. E. Wold, and J. F. Greenleaf, IEEE Trans. Med. Imaging **23**, 307 (2004).
[21] W. L. Nyborg, "Acoustic streaming," in *Nonlinear Acoustics* edited by M. F. Hamilton and D. T. Blackstock (Academic Press, San Diego, 1998), Chap. 7, pp. 215–216.
[22] L. D. Landau and E. M. Lifshitz, *Fluid Mechanics*, 2nd ed. (Butterworth-Heinemann, Oxford, 1987), Chap. 20, p. 61.